Polyhedron 46 (2012) 25–32

Contents lists available at SciVerse ScienceDirect

Polyhedron

journal homepage: www.elsevier.com/locate/poly

1-Alkyl-2-{(*o*-thioalkyl)phenylazo}imidazole complexes of mercury(II) and their photochromic properties

S. Saha (Halder) [a,1], P. Raghavaiah [b], C. Sinha [a,*]

[a] *Department of Chemistry, Inorganic Chemistry Section, Jadavpur University, Kolkata 700 032, India*
[b] *School of Chemistry, National Single Crystal X-ray Diffractometer Facility, University of Hyderabad, Hyderabad 500 046, India*

ARTICLE INFO

Article history:
Received 23 May 2012
Accepted 8 July 2012
Available online 27 July 2012

Keywords:
Hg(II)-thioalkylphenyl-azoimidazoles
X-ray structure
Photochromism
Activation energy
Effect of halide

ABSTRACT

The reaction of HgX_2 (X = Cl, Br, I) with 1-alkyl-2-{(*o*-thioalkyl)phenylazo}imidazole (SRaaiNR′) in MeOH-ethyleneglycol mixture has synthesised [Hg(SRaaiNR′)X_2]. The structure of the products has been established by microanalytical and spectral (IR, UV–Vis, ^{1}H NMR) data, and a distorted Td-geometry has been confirmed by a single crystal X-ray diffraction study of [Hg(SMeaaiNEt)I_2] (SMeaaiNEt = 1-ethyl-2-{(*o*-thiomethyl)phenylazo}imidazole). The UV light irradiation in CH_3CN solution of the complexes shows *E*-to-*Z* (*E* and *Z* refer to *trans* and *cis*-configurations) isomerisation of the coordinated SRaaiNR′ ligand about the –N=N– bond. The rate of isomerisation follows: [Hg(SRaaiNR′)Cl_2] < [Hg(SRaaiNR′)Br_2] < [Hg(SRaaiNR′)I_2]. The quantum yields ($\phi_{E\rightarrow Z}$) of the isomerisation of the complexes are lower than those of the free ligands. These may be due to increased mass and rotor volume of the complexes. The electronegativity sequence of X (I < Br < Cl) may regulate the molecular association and hence the effective mass of the rotor and the photoisomerisation rates. Thermal isomerisation determines the rate, activation energy (E_a), activation enthalpy (ΔH^*) and activation entropy (ΔS^*) of the Z → E transformation of the coordinated SRaaiNR′. The E_as of the thermal isomerisation of the complexes are lower than those of the free ligands.

1. Introduction

The color change of molecules upon light irradiation has been defined as “photochromism” by Hirshberg in 1950 [1] [from the Greek words: *phos* (light) and *chroma* (color)]. This field has been expanded since the 1960s [2–8]. Silver halide, iron, cobalt, manganese, copper, gold and a mixture of lanthanide compounds have been used as inorganic photochromes. The important problem of inorganic photochromes is “fatigue” and low durability. Numerous organic photochromes have been synthesized, which include spiropyrans, diarylethenes, quinones, azobenzenes, azopyridines, etc. However, organic photochromes suffer photodamage after several cycles of UV light irradiation. Use of metal complexes as photochromes gives increased durability, reversibility and resistance to photodegradation, photobleaching, photooxidation, etc., and also increased storing capacity. Azo compounds are important colouring agents in the dye industry and have significant capacity to coordinate to metal ions [9–11]. Hartley reported the *cis–trans* isomerisation of aromatic azo dyes in 1937 upon irradiation with UV light [12,13], and subsequently a large volume of work has been reported on derivatives of azobenzene, which are amongst the best characterized photoswitches [3,9,14–18]. Brown and Granneman had reported in 1975 [19] the isomerisation of phenylazopyridines and symmetrical azopyridines. The advantage of azopyridine derivatives is their coordination to a metal ion and hydrogen bonding through the pyridyl-N and the azo group itself. The implantation of pyridyl-N on nano particles/composite surfaces brings enormous opportunity to light driven communication in nanoscience and nanotechnology. It is expected that the coordination of ligands to metal ions drifts the charge from the ligand, and hence influences the electron density. This affects the electronic, physical and chemical properties of the compounds, and even induces some chemical transformations that are otherwise impossible. The coordination of metal ions to organic photochromes may affect the isomerisation properties, rates and conversion efficiency [20,21]. The exploration of photoswitching of other azoheterocycles is an exciting area of research. The first report of photoisomerisation of phenylazoimidazole appeared in 2003 [22] by Majima and co-workers and a subsequent publication appeared in 2005 by Otsuki et al. [23]. Phenylazoimidazoles constitute an interesting class of compounds in coordination chemistry that are important in biological applications since imidazole is a ubiquitous and essential group in biology, especially as a metal coordinating site. The photochromism of 1-alkyl-2-(arylazo)imidazoles (RaaiNR′) [23,24] and some of their metal complexes [25–28] have

---

* Corresponding author.
E-mail address: c_r_sinha@yahoo.com (C. Sinha).

[1] Present address: Kalyani Govt. Engg. College, Kalyani, Nadia, West Bengal 741 235, India.

0277-5387/$ - see front matter © 2012 Elsevier Ltd. All rights reserved.
http://dx.doi.org/10.1016/j.poly.2012.07.063

Table 1
Summarized crystallographic data for [Hg(SMeaaiNEt)I$_2$] (**5b**).

	5b
Empirical formula	$C_{12}H_{14}N_4I_2SHg$
Formula weight	700.73
Temperature (K)	100(2)
Crystal system	Monoclinic
Space group	$P21/n$
Crystal size (mm)^3	0.10 × 0.15 × 0.20
a (Å)	12.3065(14)
b (Å)	11.9461(17)
c (Å)	12.6300(18)
α (°)	90.00
β (°)	112.170(5)
γ (°)	90.00
V (Å)^3	1719.5(4)
Z	4
μ (Mo Kα) (mm^{-1})	12.7
θ range	1.97–28.71
hkl range	$-16 < h < 15$; $-16 < k < 16$; $-17 < l < 17$
D_{calc} (mg m^{-3})	2.707
Refine parameters	183
Total reflections	19575
Unique reflections	4445
R_1[a] [$I > 2\sigma(I)$]	0.0332
wR_2[b]	0.0913
Goodness of fit	1.04

[a] $R = \sum||F_o| - |F_c||/\sum|F_o|$.

[b] $wR_2 = [\sum w(F_o^2 - F_c^2)^2/\sum w(F_o^2)^2]^{1/2}$, $w = 1/[\sigma^2(F_o)^2 + (0.0356P)^2]$ for **5b**; where $P = (F_o^2 + 2F_c^2)/3$.

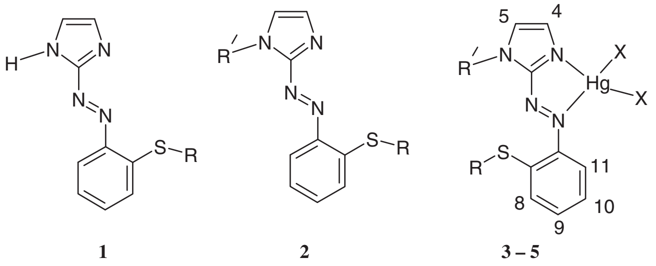

Scheme 1. The ligands SRaaiNR′ and the mercury(II) complexes Hg(SRaaiNR′)X$_2$ (X = Cl (**3**), Br (**4**), I (**5**) R = R′ = Me (**a**); R = Me, R′ = Et (**b**); R = Et, R′ = Me (**c**); R = R′ = Et (**d**)).

inspired us to examine the photochromism of other transition and non-transition metal complexes. In this work we have used 1-alkyl-2-{(*o*-thioalkyl)phenylazo}imidazole (SRaaiNR′), a flexidentate ligand–tridentate (N,N′,S) [29]/bidentate (N,N′) [30]/monodentate N [31] (where N, N′, S refer to N(imidazolyl), N(azo) and –S-R donor centres, respectively), to synthesise Hg(II) complexes using different halides (X = Cl, Br, I) as neutralizing charges. The complexes have been spectroscopically (FT-IR, UV–Vis, ^{1}H NMR) characterized and in one case single crystal X-ray diffraction has been used for the structural confirmation. The photoisomerisation of coordinated SRaaiNR′ (*E* (*trans*) → *Z* (*cis*)) has been monitored by UV light irradiation and the rates and quantum yields have been determined; the effect of coordination of SRaaiNR′ to Hg(II), the influence of X in the complexes etc. are accounted for in this work.

2. Experimental

2.1. Material

$HgCl_2$, $HgBr_2$ and HgI_2 were obtained from Loba Chemicals, Bombay, India. 1-Alkyl-2-{(*o*-thioalkyl)phenylazo}imidazole were synthesized by a reported procedure [29]. All other chemicals and solvents were reagent grade as received.

2.2. Physical measurements

Microanalytical data (C, H, N) were collected on a Perkin-Elmer 2400 CHNS/O elemental analyzer. Spectroscopic data were obtained using the following instruments: UV–Vis spectra from a Perkin Elmer Lambda 25 spectrophotometer; IR spectra (KBr disk, 4000–200 cm^{-1}) from a Perkin Elmer RX-1 FTIR spectrophotometer; photoexcitation has been carried out using a Perkin Elmer LS-55 spectrofluorimeter and ^{1}H NMR spectra from a Bruker (AC) 300 MHz FTNMR spectrometer.

2.3. Synthesis of [Hg(SMeaaiNEt)I$_2$] (*5b*)

1-Ethyl-2-{(*o*-thiomethyl)phenylazo}imidazole (16.30 mg, 0.066 mmol) in CH_3OH was added in drops to a MeOH–ethyleneglycol (4:1, v/v) solution of HgI_2 (30 mg, 0.066 mmol) and the resulting mixture was stirred for 2 h. The resultant red solution was collected after filtration. Slow evaporation of the solution crystallized a red compound. The yield was 30.98 mg (67%). The other complexes were prepared following identical reaction conditions and the yield varied in the range 60–70%.

Data of the complexes are as follows: [Hg(SMeaaiNMe)Cl$_2$] (**3a**) *Anal.* Calc. for $C_{11}H_{12}N_4SCl_2Hg$: C, 26.22; H, 2.40; N, 11.12. Found: C, 26.20; H, 2.42; N, 11.15%. FT-IR (KBr disc, cm^{-1}): ν(N=N) 1424; ν(C=N) 1505. UV–Vis spectroscopic data in CH_3CN (λ_{max} (nm) (10^{-3} $\in$ (dm^3 mol^{-1} cm^{-1}))): 379 (13.83), 416 (10.71). [Hg(SMeaaiNEt)Cl$_2$] (**3b**) *Anal.* Calc. for $C_{12}H_{14}N_4SCl_2Hg$: C, 27.83; H, 2.72; N, 10.81. Found: C, 27.78; H, 2.74; N, 10.84%. FT-IR (KBr disc, cm^{-1}): ν(N=N) 1424; ν(C=N) 1512. UV–Vis spectroscopic data in CH_3CN (λ_{max} (nm) (10^{-3} $\in$ (dm^3 mol^{-1} cm^{-1}))): 380 (12.18), 417 (9.52). [Hg(SEtaaiNMe)Cl$_2$] (**3c**) *Anal.* Calc. for $C_{12}H_{14}$-

Table 2
^{1}H NMR spectral data of [Hg(SRaaiNR′)X$_2$] in $CDCl_3$.

	δ, ppm (J, Hz)										
	4-H^{bs}	5H^{bs}	8H^d	9,10-H^m	11-H^d	N(1)–CH$_3$^{s}	N(1)–CH$_2$^{q}	[N(1)CH$_2$–] CH$_3$^{t}	S–CH$_3$^{s}	S–CH$_2$^{q}	[S–CH$_2$–] CH$_3$^{t}
[Hg(SMeaaiNMe)Cl$_2$] (**3a**)	7.38	7.27	7.35 (7.4)	7.59	7.95 (8.1)	4.20			2.68		
[Hg(SMeaaiNEt)Cl$_2$] (**3b**)	7.40	7.22	7.34 (7.4)	7.58	7.97 (8.2)		4.66 (7.3)	1.69 (8.0)	2.67		
[Hg(SEtaaiNMe)Cl$_2$] (**3c**)	7.35	7.20	7.30 (7.8)	7.58	7.97 (8.2)	4.19				3.19 (7.0)	1.45 (8.0)
Hg(SEtaaiNEt)Cl$_2$] (**3d**)	7.39	7.27	7.31 (7.8)	7.59	7.96 (8.2)		4.58 (7.3)	1.65 (8.0)		3.18 (7.0)	1.46 (8.0)
[Hg(SMeaaiNMe)Br$_2$] (**4a**)	7.38	7.23	7.34 (8.0)	7.58	7.94 (8.0)	4.17			2.66		
[Hg(SMeaaiNEt)Br$_2$] (**4b**)	7.39	7.21	7.33 (7.8)	7.56	7.96 (8.1)		4.57 (7.3)	1.63 (8.0)	2.62		
[Hg(SEtaaiNMe)Br$_2$] (**4c**)	7.41	7.23	7.30 (7.8)	7.55	7.95 (8.0)	4.16				3.19 (7.0)	1.45 (8.0)
[Hg(SEtaaiNEt)Br$_2$] (**4d**)	7.39	7.20	7.35 (8.0)	7.58	7.96 (8.1)		4.55 (7.3)	1.64 (8.0)		3.18 (7.0)	1.44 (8.0)
[Hg(SMeaaiNMe)I$_2$] (**5a**)	7.36	7.19	7.33 (8.0)	7.57	7.93 (8.0)	4.16			2.63		
[Hg(SMeaaiNEt)I$_2$] (**5b**)	7.37	7.20	7.37 (7.5)	7.54	7.90 (7.9)		4.55 (7.3)	1.66 (8.0)	2.61		
[Hg(SEtaaiNMe)I$_2$] (**5c**)	7.38	7.23	7.37 (7.8)	7.53	7.87 (7.9)	4.14				3.18 (7.0)	1.46 (8.0)
[Hg(SEtaaiNEt)I$_2$] (**5d**)	7.37	7.20	7.38 (8.00)	7.58	7.90 (8.0)		4.52 (7.3)	1.62 (8.0)		3.24 (7.0)	1.43 (8.0)

^{bs}Broad singlet; ^{d}doublet; ^{m}multiplet; ^{s}singlet; ^{t}triplet; ^{q}quartet.

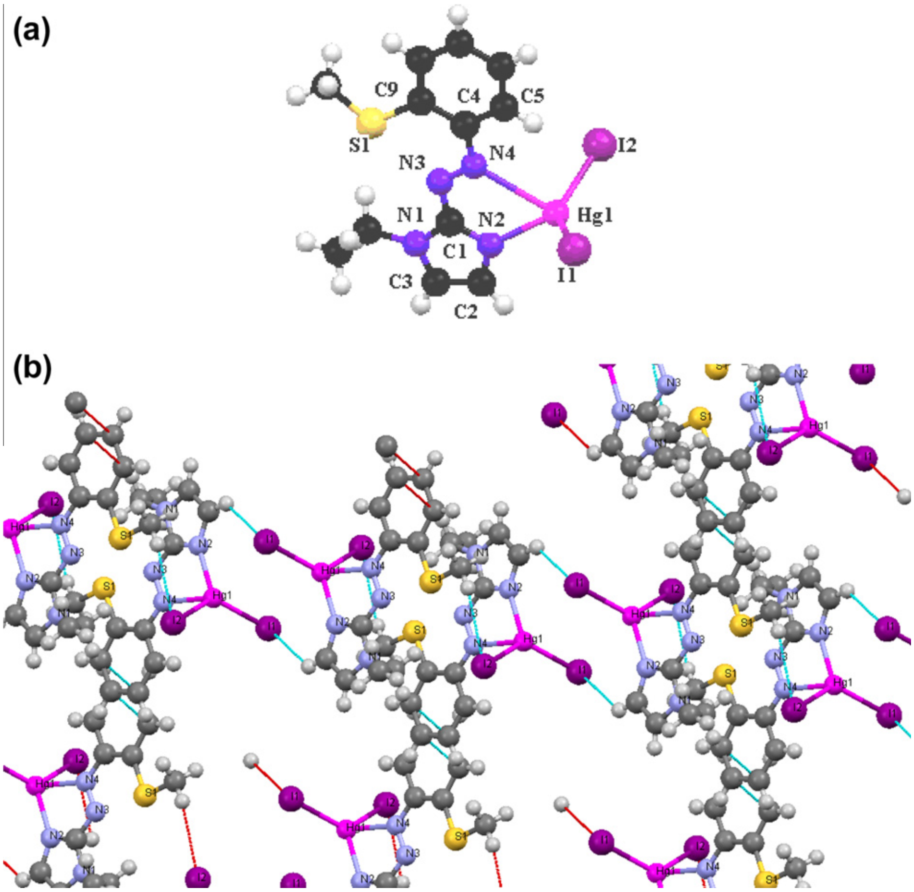

Fig. 1. Crystal structure of (a) [Hg(SMeaaiNEt)I$_2$] (**5b**) and (b) 1D chain structure constituted by C–H···I hydrogen bonds and π···π interactions.

Table 3
Selected bond distances and bond angles of the compound Hg(SMeaaiNEt)I$_2$ (**5b**).

	Bond distance (Å)		Bond angle (°)
Hg(1)–I(1)	2.6826(6)	I(1)–Hg(1)–I(2)	128.475(16)
Hg(1)–I(2)	2.6467(6)	I(1)–Hg(1)–N(2)	112.11(12)
Hg(1)–N(2)	2.297(5)	I(2)–Hg(1)–N(2)	119.21(12)
N(3)–N(4)	1.271(6)	Hg(1)–N(2)–C(1)	120.2(4)
Hg(1)–N(4)	2.780(4)	Hg(1)–N(2)–C(2)	134.3(4)
Hg(1)···Hg(1a)	4.330	N(2)–Hg(1)–N(4)	64.29(15)
Hg(1)···I(1a)	3.581	I(2)–Hg(1)–N(4)	96.98(9)
		I(1)–Hg(1)–N(4)	101.08(9)
		N(3)–N(4)–Hg(1).	112.5(3)
		C(4)–N(4)–Hg(1).	131.8(3)

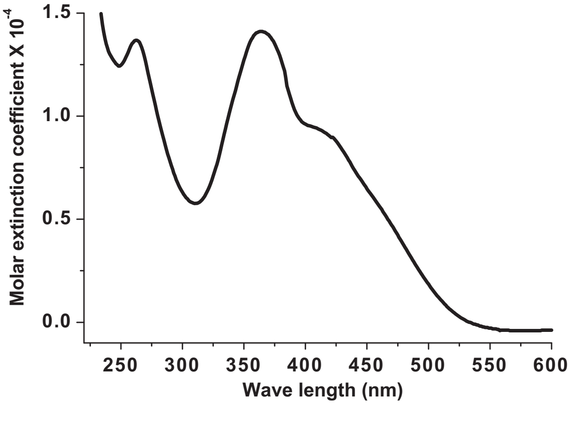

Fig. 2. UV–Vis spectrum of [Hg(SMeaaiNEt)I$_2$] (**5b**) in CH$_3$CN at 27 °C.

N$_4$SCl$_2$Hg: C, 27.83; H, 2.72; N, 10.81. Found: C, 27.82; H, 2.73; N, 10.82%. FT-IR (KBr disc, cm^{-1}): ν(N=N) 1423; ν(C=N) 1504. UV–Vis spectroscopic data in CH$_3$CN (λ_{max} (nm) (10^{-3} $\in$ (dm^3 mol^{-1} cm^{-1}))): 379 (13.01), 418 (9.12). [Hg(SEtaaiNEt)Cl$_2$] (**3d**) *Anal.* Calc. for C$_{13}$H$_{16}$N$_4$SCl$_2$Hg: C, 29.36; H, 3.03; N, 10.53. Found: C, 29.37; H, 3.03; N, 10.50%. FT-IR (KBr disc, cm^{-1}): ν(N=N) 1424; ν(C=N) 1511. UV–Vis spectroscopic data in CH$_3$CN (λ_{max} (nm) (10^{-3} $\in$ (dm^3 mol^{-1} cm^{-1}))): 380 (12.91), 417 (9.22). [Hg(SMeaaiNMe)Br$_2$] (**4a**) *Anal.* Calc. for C$_{11}$H$_{12}$N$_4$SBr$_2$Hg: C, 22.29; H, 2.04; N, 9.45. Found: C, 22.25; H, 2.05; N, 9.46%. FT-IR (KBr disc, cm^{-1}): ν(N=N) 1423; ν(C=N) 1500. UV–Vis spectroscopic data in CH$_3$CN (λ_{max} (nm) (10^{-3} $\in$ (dm^3 mol^{-1} cm^{-1}))): 369 (12.31), 419 (9.52). [Hg(SMeaaiNEt)Br$_2$] (**4b**) *Anal.* Calc. for C$_{12}$H$_{14}$N$_4$SBr$_2$Hg: C, 23.75; H, 2.32; N, 9.23. Found: C, 23.77; H, 2.31; N, 9.20%. FT-IR (KBr disc, cm^{-1}): ν(N=N) 1422; ν(C=N) 1508. UV–Vis spectroscopic data in CH$_3$CN (λ_{max} (nm) (10^{-3} $\in$ (dm^3 mol^{-1} cm^{-1}))): 368 (13.11), 420 (8.34). [Hg(SEtaaiNMe)Br$_2$] (**4c**) *Anal.* Calc. for C$_{12}$H$_{14}$N$_4$SBr$_2$Hg: C, 23.75; H, 2.32; N, 9.23. Found: C, 23.72; H, 2.29; N, 9.22%. FT-IR (KBr disc, cm^{-1}): ν(N=N) 1421; ν(C=N) 1499. UV–Vis spectroscopic data in CH$_3$CN (λ_{max} (nm) (10^{-3} $\in$ (dm^3 mol^{-1} cm^{-1}))): 369 (12.12), 418 (8.25). [Hg(SEtaaiNEt)Br$_2$] (**4d**) *Anal.* Calc. for C$_{13}$H$_{16}$N$_4$SBr$_2$Hg: C, 25.15; H, 2.59; N, 9.02. Found: C, 25.10; H, 2.60; N, 9.00%. FT-IR (KBr disc, cm^{-1}): ν(N=N) 1422; ν(C=N) 1509. UV–Vis spectroscopic data in CH$_3$CN (λ_{max} (nm) (10^{-3} $\in$ (dm^3 mol^{-1} -cm^{-1}))): 369 (12.90), 419 (8.36). [Hg(SMeaaiNMe)I$_2$] (**5a**) *Anal.* Calc. for C$_{11}$H$_{12}$N$_4$SI$_2$Hg: C, 19.24; H, 1.76; N, 8.16. Found: C, 19.26; H, 1.70; N, 8.18%. FT-IR (KBr disc, cm^{-1}): ν(N=N) 1416; ν(C=N) 1498. UV–Vis spectroscopic data in CH$_3$CN (λ_{max} (nm)

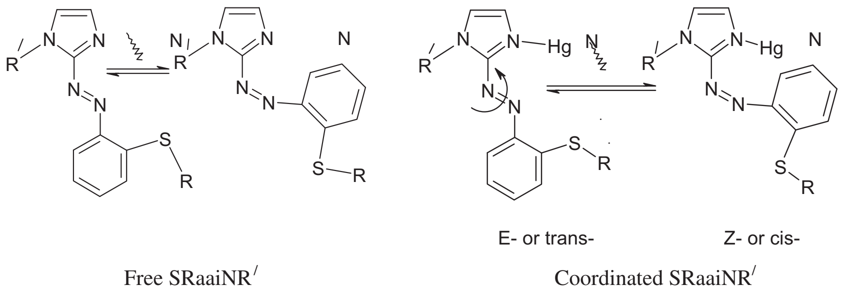

Scheme 2. Photochromism of free and coordinated SRaaiNR′.

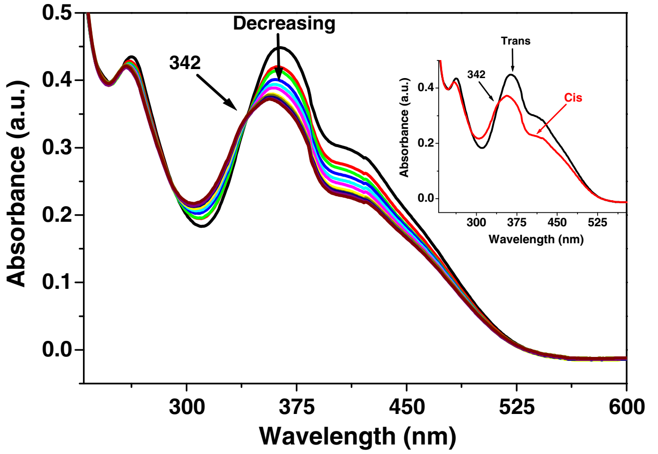

Fig. 3. Spectral changes of $[Hg(SMeaaiNEt)I_2]$ (**5b**) in MeCN upon repeated light irradiation at 364 nm at 4 min interval at 25 °C. Inset shows the *trans* (*E*) and *cis* (*Z*) isomeric spectra.

Table 4
Excitation wavelength ($\lambda_{\pi,\pi*}$), rate of *E* (*trans*) → *Z* (*cis*) conversion and quantum yield ($\phi_{E\to Z}$).

Compound	$\lambda_{\pi,\pi*}$ (nm)	Isosbestic points (nm)	Rate of $E \to Z$ conversion ($\times 10^8\ s^{-1}$)	$\phi_{E\to Z}$
2a[a]	357	337	4.908	0.317
2b[a]	358	337	3.108	0.232
2c[a]	357	336	4.67	0.290
2d[a]	356	335	2.948	0.197
3a	360	337	3.61	0.235
3b	361	340	2.30	0.173
3c	362	341	3.1	0.187
3d	362	339	2.12	0.121
4a	361	338	3.89	0.258
4b	362	341	2.51	0.19
4c	363	340	3.39	0.22
4d	362	339	2.42	0.151
5a	361	338	4.11	0.288
5b	364	342	2.79	0.202
5c	363	343	3.75	0.261
5d	362	340	2.62	0.168

[a] Received from Ref. [25].

$(10^{-3} \in (dm^3\ mol^{-1}\ cm^{-1})))$: 364 (12.56), 428 (7.14). $[Hg(SMeaaiNEt)I_2]$ (**5b**) *Anal.* Calc. for $C_{12}H_{14}N_4SI_2Hg$: C, 20.57; H, 2.01; N, 7.99. Found: C, 20.59; H, 2.03; N, 7.94%. FT-IR (KBr disc, cm^{-1}): ν(N=N) 1421; ν(C=N) 1494. UV–Vis spectroscopic data in CH_3CN (λ_{max} (nm) $(10^{-3} \in (dm^3\ mol^{-1}\ cm^{-1})))$: 363 (13.34), 431 (7.89). $[Hg(SEtaaiNMe)I_2]$ (**5c**) *Anal.* Calc. for $C_{12}H_{14}N_4SI_2Hg$: C, 20.57; H, 2.01; N, 7.99. Found: C, 20.55; H, 2.03; N, 7.95%. FT-IR (KBr disc, cm^{-1}): ν(N=N) 1424; ν(C=N) 1497. UV–Vis spectroscopic data in CH_3CN (λ_{max} (nm) $(10^{-3} \in (dm^3\ mol^{-1}\ cm^{-1})))$: 363 (12.054), 424 (7.12). $[Hg(SEtaaiNEt)I_2]$ (**5d**) *Anal.* Calc. for $C_{13}H_{16}N_4SI_2Hg$: C, 21.84; H, 2.25; N, 7.84. Found: C, 21.86; H, 2.22; N, 7.85%. FT-IR (KBr disc, cm^{-1}): ν(N=N) 1423; ν(C=N) 1496. UV–Vis spectroscopic data in CH_3CN (λ_{max} (nm) $(10^{-3} \in (dm^3\ mol^{-1}\ cm^{-1})))$: 364 (12.84), 427 (7.45).

2.4. X-ray diffraction study

The single crystals suitable for data collection were grown from slow evaporation of a CH_3CN solution of the complexes. The crystal data and details of the data collections are given in Table 1. A suitable single crystal of **5b** was mounted on a Bruker SMART APEX CCD diffractometer (graphite monochromated Mo Kα radiation, $\lambda = 0.71073$ Å) and data were collected by use of ω scans. Unit cell parameters were determined from least-squares refinement of setting angles (θ) within the range $1.97° \leqslant \theta \leqslant 28.71°$. Out of 19575 collected data, 4445 with $I > 2\sigma(I)$ were used for the structure solution. The *hkl* ranges were $-16 \leqslant h \leqslant 15$, $-16 \leqslant k \leqslant 16$, $-17 \leqslant l \leqslant 17$. Data were corrected for Lorentz polarization effects and for linear decay. Semi-empirical absorption corrections based on ψ-scans were applied. The structure were solved by direct method using SHELXS-97 [32] and successive difference Fourier syntheses. All non-hydrogen atoms were refined anisotropically. The hydrogen atoms were fixed geometrically and refined using the riding model. All calculations were carried out using SHELXL-97 [33], ORTEP-32 [34] and PLATON-99 [35] programs.

3. Results and discussion

3.1. Synthesis of the complexes

The ligands were synthesized by coupling the *o*-(thioalkyl)phenyldiazonium ion with imidazole in sodium carbonate solution, and purified by solvent extraction and chromatographic processes [29]. The alkylation of 2-[*o*-(thioalkyl)phenylazo]imidazole (**1**) has been carried out by adding alkyl iodide (MeI, EtI) in dry THF solution in the presence of NaH and the 1-alkyl-2-{(*o*-thioalkyl)phenylazo}imidazoles [SRaaiNR′ (R = R′ = Me (**2a**); R = Me, R′ = Et (**2b**); R = Et, R′ = Me (**2c**); R = R′ = Et (**2d**))] were purified by chromatography.

The reaction of HgX_2 (X = Cl, Br, I) and SRaaiNR′ in MeOH–ethyleneglycol (4:1 v/v) isolates the crystalline compounds $[Hg(SRaaiNR')X_2]$ (**3–5**). The composition of the complexes has been confirmed by microanalytical data and by other spectroscopic information. The structure has been established in the case of $[Hg(SMeaaiNEt)I_2]$ (**5b**) by single-crystal X-ray diffraction studies.

3.2. Infrared and ^1H NMR spectra

The infrared spectra of the compounds in KBr discs show moderately intense stretches at 1500–1515 and 1415–1425 cm^{-1} which are assigned to ν(C=N) and ν(N=N), respectively. Other vibrations are shifted to lower frequency in the complexes

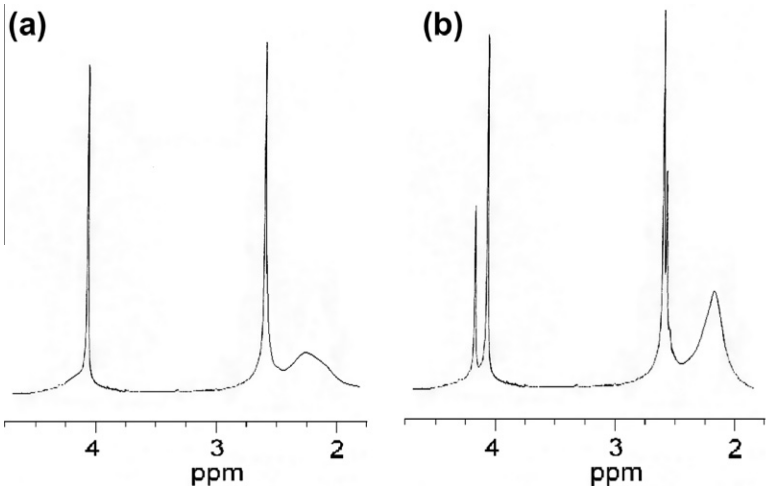

Fig. 4. ^{1}H NMR spectra of the aliphatic region of [Hg(SMeaaiNMe)Cl_2] (**3a**) in CD_3CN (a) before irradiation and (b) after irradiation of UV light at 360 nm for 20 min.

compared to the free ligand values [29]. The ^{1}H NMR spectra are recorded in $CDCl_3$ (Table 2). The atom numbering pattern is shown in Scheme 1. The N(1)–Me signal appears as a singlet at 4.14–4.20 ppm; N–CH_2–CH_3 shows a quartet for –CH_2– at *ca.* 4.52–4.66 (7.3 Hz) and a triplet at 1.62–1.69 (8.0 Hz) ppm. The thioalkyl group S–R also exhibits a singlet signal at 2.61–2.68 ppm for S–Me of SMeaaiNR′ (**3a**,**b**–**6a**,**b**). SEtaaiNEt (**3d**–**6d**) shows quartets (4.5 (7 Hz) and 3.00 (7 Hz) ppm for the –CH_2– protons of N–CH_2–(CH_3) and S–CH_2–(CH_3), respectively) and triplets (at 1.6 and 1.4 ppm for –(N–CH_2)–CH_3 and –(S–CH_2)CH_3, respectively). Imidazole 4- and 5-H appears as a broad singlet at 7.35–7.41 and 7.19–7.27 ppm, respectively. Broadening may be due to rapid proton exchange between these imidazole protons. The aryl protons, 8-H to 11-H (7.3–7.9 ppm), reveal that the signals in the spectra of the complexes are shifted downfield relative to the free ligand values.

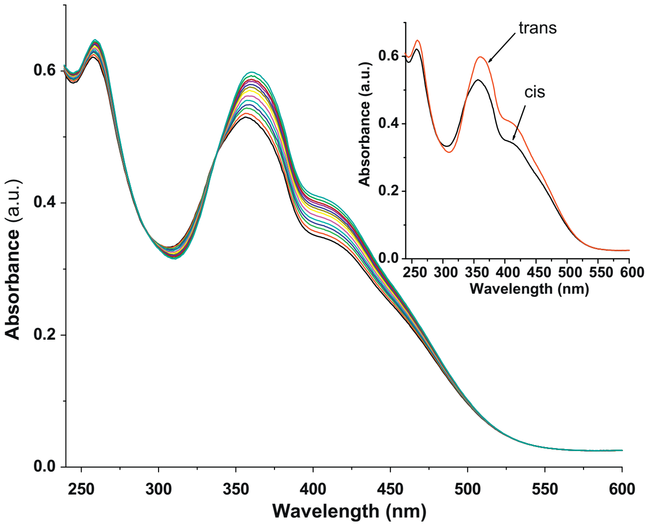

Fig. 5. Thermal isomerisation, *Z* (*cis*) → *E* (*trans*) of [Hg(SMeaaiNEt)I_2] (**5b**) in MeCN at 4 min interval at 25 °C (inset shows spectra of cis- and trans isomers).

3.3. Molecular structure of [Hg(SMeaaiNEt)I_2] (5b)

The crystals of [Hg(SMeaaiNEt)I_2] (**5b**) were obtained by slow evaporation of CH_3CN solution under ambient conditions. The molecular structure is shown in Fig. 1 and selected bond parameters are listed in Table 3. Each discrete molecular unit consists of a HgN_2I_2 coordination sphere where SMeaaiNEt acts as N,N′-chelating agent (N and N′ refer to N(imidazole) and N(azo) donor centres), although it has three potential N,N′,S donor centres. The S-Me moiety remains uncoordinated and stereochemically away from the Hg(II) centre. The atomic arrangement of Hg(1), N(4), N(3), C(1) and N(2) constitute the chelate plane with a maximum deviation <0.04 Å. The pendant phenyl ring makes a small dihedral of 4.7° with the chelated azoimidazole ring. The small chelate angle (64.29(15)°) may be one of the reasons for geometrical distortion. The Hg–N(imidazole) distance (Hg(1)–N(1), 2.297(5) Å) is shorter than that of Hg–N(azo) (Hg(1)–N(4), 2.780(4) Å), which reflects the stronger interaction between Hg(II) and N(imidazole). Although the Hg–N(azo) bond length is very long, it is less than the sum of the van der Waals radii of Hg(II) (1.55 Å) and N(sp^2) (1.53 Å). This implies a significant bonding interaction between these components. The stronger coordination of imidazole-N to Hg(II) compared to azo-N has a significant biochemical implication and explains the strong toxicity of Hg(II). Because of the long Hg(II)–N(azo) distance, the molecule is useful for photo-activation *via* cleavage of this bond followed by rotation to introduce photo-isomerisation (*vide infra*). The N=N distance is 1.271(6) Å and is longer than the free ligand data [24]. The bond parameters are in good agreement with previously reported structures of Hg(II)-{1-alkyl-(2-arylazo)imidazole}iodide [27]. The non-covalent interaction of –SEt–C_6H_4– such as [Cg(2) (molecule A)···Cg(2a) (molecule B) is 3.370 Å (Cg(2/2a)–C(4)–C(5)–C(6)–C(7)–C(8)–C(9)); symmetry, 2 − *x*, 1 − *y*, 2 − *z*]. A weak hydrogen bonding is also observed at C(7)–H(7)···Cg(1) [H(7)···Cg(1), C(7)···Cg(1) and ∠C(7)–H(7)···Cg(1) are 2.768, 3.648 Å and 154.46°, respectively where Cg(1) is N(1)–C(1)–N(2)–C(2)–C(3); symmetry −1/2+ *x*, 3/2 − *y*, 1/2 + *z*] and C(11)–H(11)···Cg(2) [H(11)···Cg(2), C(11)···Cg(2) and ∠C(11)–H(11)···Cg(2) are 3.380, 4.353 Å and 171.95°, respectively; symmetry −3/2 − *x*, 1/2+ *y*, 3/2 − *z*]. Iodine is also hydrogen bonded to form a 1D chain, C(2)–H(2)···I(1) where H(2)···I(1), 3.08(2) Å; C(2)···I(1), 3.77(9) Å and ∠C(2)–H(2)···I(1), 131.54° (Fig. 1b).

3.4. UV–Vis spectra and photochromism

The electronic spectra were taken in CH_3CN solution. Two main bands are observed in the UV –Vis region. On comparing with the free ligands spectra [27] and that of Hg(II) complexes, we may conclude that these bands come from intramolecular charge-transfer

Table 5
Rate and activation parameters for Z (*cis*) → E (*trans*) thermal isomerisation.

Compound	Temperature (K)	Rate thermal c → t conversion ($\times 10^4$ s^{-1})	E_a (kJ mol^{-1})	ΔH^* (kJ mol^{-1})	ΔS^* (J mol^{-1} K^{-1})	ΔG^* (kJ mol^{-1})
2a[a]	298	4.329	25.42	22.88	−232.41	92.13
	303	5.295				93.29
	308	6.191				94.45
	313	7.091				95.62
2b[a]	298	4.614	22.99	20.45	−240.02	91.97
	303	5.598				93.17
	308	6.293				94.37
	313	7.269				95.57
2c[a]	298	4.425	21.92	19.38	−244.04	92.11
	303	5.123				93.33
	308	5.985				94.55
	313	6.729				95.77
2d[a]	298	4.625	18.88	16.34	−253.96	92.02
	303	5.123				93.29
	308	5.985				94.56
	313	6.589				95.83
3a	304	7.82	15.68	13.09	−261.68	79.56
	309	8.33				80.87
	314	8.855				82.18
	319	10.6				83.49
3b	304	8.18	13.66	11.07	−267.91	81.45
	309	8.7				82.79
	314	9.1				84.13
	319	10.7				85.47
3c	304	8.25	13.75	11.16	−267.55	81.35
	309	8.77				82.69
	314	9.2				84.02
	319	10.8				85.36
3d	304	8.63	11.8	9.21	−273.54	83.16
	309	9.1				84.53
	314	9.67				83.16
	319	10.8				87.27
4a	304	8.23	17.4	14.81	−255.58	77.71
	309	8.82				78.99
	314	9.79				80.27
	319	11.4				81.54
4b	304	8.45	16.29	13.7	−258.91	78.72
	309	9.26				80.02
	314	10.1				81.31
	319	11.5				82.61
4c	304	8.49	16.6	14.01	−257.85	78.40
	309	9.28				79.69
	314	10.2				80.98
	319	11.6				82.27
4d	304	8.94	14.45	11.86	−264.53	80.43
	309	9.65				81.75
	314	10.3				83.07
	319	11.8				84.34
5a	304	8.28	19.29	16.71	−249.31	75.80
	309	8.9				77.05
	314	10.2				78.3
	319	11.8				79.55
5b	304	8.5	17.69	15.1	−254.31	77.33
	309	9.18				78.6
	314	10.3				79.87
	319	11.8				81.14
5c	304	8.54	17.99	15.40	−253.3	77.02
	309	9.2				78.28
	314	10.4				79.55
	319	11.9				80.82
5d	304	8.99	14.82	12.23	−263.33	80.06
	309	9.5				81.38
	314	10.3				82.7
	319	11.9				84.01

[a] Received from Ref. [25].

transitions (n → π*, π → π*). The complexes show a structured absorption band around 360–390 nm with a molar absorption coefficient ($\in \sim 10^3$ M^{-1} cm^2) and a weak band at 415–420 nm ($\in \sim 10^3$ M^{-1} cm^2) (Fig. 2). From the analogous absorption spectra of the ligands, it is concluded that the absorption band around 360–380 nm corresponds to π–π* transitions, while the tail corresponds to an admixture of n–π* and Hg(II) → π*(azoimine) transitions.

The UV-light irradiation at a fixed time interval at 360–390 nm to a CH_3CN solution of the ligands shows changes in the absorption spectra that corresponds to a structural change of the ligand from *trans*-SRaaiNR′ (*E*-isomer) to *cis*-SRaaiNR′ (*Z*-isomer) (Scheme 2, Fig. 3). The intense peak in the UV zone decreases with a slight increase in the tail portion of the spectra in the visible region, until a stationary state is reached. The irradiation at the newly appearing longer wavelength peak (∼420 nm) reverses the process very slowly and the original spectra are recovered. The quantum yields of the *E*-to-*Z* photoisomerization are given in Table 4. It is observed that upon irradiation with UV light, the *E*-to-*Z* change proceeds and the *Z* molar ratio reaches ∼85%. The absorption spectra of the coordinated SRaaiNR′ ligands in the *E*-form change upon excitation (Fig. 3) into the *Z*-isomer. The ligands and the complexes show little sign of degradation upon repeated irradiation for up to at least 15 cycles in each case. The quantum yields were measured for the *E*-to-*Z* ($\phi_{E\to Z}$) acetonitrile solution on irradiation with UV light. The $\phi_{E\to Z}$ values are significantly dependent on nature of substituents. The photoisomerisation rate and quantum yields of coordinated ligands are decreased compared to the free ligands and in general, an increase in mass of the molecule reduces the rate and quantum yield of isomerisation.

The ^{1}H NMR spectra of [Hg(SMeaaiNMe)Cl_2] in CD_3CN were recorded before and after UV irradiation at 360 nm and it is observed that the aromatic ring protons are significantly shifted upfield after the light irradiation. The ^{1}H NMR spectra of the irradiated molecules show the presence of two closely associated signals of different intensity ratios, which are distinguishable in the aliphatic region of the N–Me group (Fig. 4), whilst it was difficult to analyze the aromatic region because of the complexity of overlapping proton signals. The lower intense signal, which appears at higher δ values (shifted by 0.05–0.15 ppm), may be the contribution from the *cis*-configuration of coordinated SMeaaiNMe. However, we have not carried out an NMR experiment of irradiated solution of all the complexes.

On comparing with previously reported photoisomerisation results of [Hg{1-alkyl-2-(arylazo)imidazole}(μ-X)X]$_2$ [27], we observe that the present complexes show a higher $E \to Z$ rate and better quantum yields, although the formula weight of the present molecules are higher than the earlier examples. The dimeric nature of the previous complexes may increase the rotor mass relative to the monomeric nature of the present complexes and may be a probable reason for the decrease in the rate and quantum yields. The rate and quantum yields ($\phi_{\mathrm{t}\to\mathrm{c}}$) are considerably dependent on the position of the substituents. Substitution at the imidazolyl ring (–NR) is recognizably different from –SR substitution towards the regulation of photochromism. These parameters follow the sequence [Hg(SMeaaiNMe)X_2] (**a**) > [Hg(SEtaaiNMe)X_2] (**c**) > [Hg(SMeaaiNEt)X_2] (**b**) > [Hg(SEtaaiNEt)X_2] (**d**). The –NR group has a higher mass influence than –SR, which may be due to the coordination of imidazole-N to Hg(II) in which the ring –NR is added, while the –SR group is free. Besides, the overall mass influence on the rate and photochromism is common in all these complexes. In general, an increase in mass of a molecule reduces the rate of the *trans*-to-*cis* isomerisation.

The *Z*-to-*E* isomerisation of SRaaiNR′ (**2**) and their Hg(II) complexes (**3–5**) were followed by spectral measurements in CH_3CN (Fig. 5) at various temperatures, 298–313 K. The Eyring plots in the range 298–313 K gave a linear graph from which the activation parameters E_a, ΔS^*, ΔH^* and ΔG^* were calculated (Table 5, Fig. 6). The complexes show lower E_as than that of free ligand data and that of [Hg{1-alkyl-2-(arylazo)imidazole}(μ-X)X]$_2$ [27], which means faster *Z*-to-*E* thermal isomerisation, and this indeed was observed. The entropy of activation (ΔS^*) also correlates with the E_as with regard to the progress of the thermal isomerisation of the complexes compared to the free ligands. This also supports an increase in rotor volume of the complexes. The E_as are considerably dependent on the position of substituents, like the rate and quantum yields of the *trans-to-cis* isomerisation. The E_as follow the sequence (**a**) > (**c**) > (**b**) > (**d**).

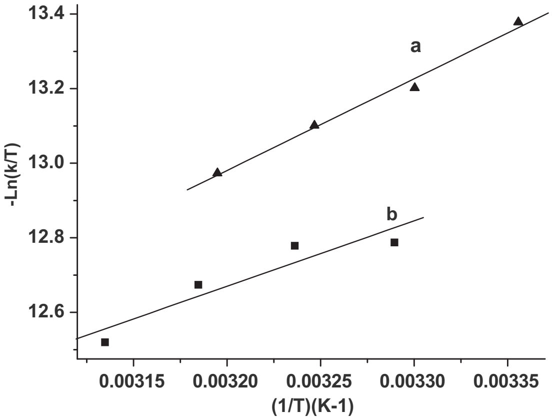

Fig. 6. The Eyring plots of rate constants of Z (*cis*) to E (*trans*) thermal isomerisation of (a) SMeaaiNEt (**2b**) and (b) [Hg(SMeaaiNEt)I_2] (**5b**) at 298, 303, 308 and 313 K.

4. Conclusion

Hg(1-alkyl-2-{(*o*-thioalkyl)phenylazo}imidazole)X_2 complexes have been characterized by spectral data and in one case by a single crystal X-ray diffraction study. The photoisomerisation of the complexes have been examined by UV light irradiation in CH_3CN solution and the results are compared with free ligand data. The decrease in electronegativity of X increases the rate of $E \to Z$ photoisomerisation. The $Z \to E$ isomerisation is a thermally driven process. The activation energies (E_as) of $Z \to E$ isomerisation have been calculated and the values are lower than the free ligand data. The slow rate of isomerisation in the complexes may be due to a higher rotor volume than that of the free ligands.

Acknowledgment

Financial support from the Department of Science and Technology, New Delhi is thankfully acknowledged.

References

[1] Y. Hirshberg, Compt. Rend. Acad. Sci. (Paris) 231 (1950) 903.
[2] G.H. Brown (Ed.), Photochromism, Wiley–Intersciences, New York, 1971.
[3] H. Rau, in: H. Durr, H. Bouas-Laurent (Eds.), Photochromism: Molecules and Systems, Elsevier, Amsterdam, 1990.
[4] B.L. Feringa (Ed.), Molecular Switches, Wiley-VCH, Weinheim, 2001.
[5] R.C. Bertelson, in: G.H. Brown (Ed.), Photochromism, Wiley, New York, 1971, p. 45.
[6] R. Guglielmetti, in: H. Dürr, H. Bouas-Laurent (Eds.), Photochromism: Molecules and Systems, Elsevier, Amsterdam, 1990, p. 314, 855.
[7] I. Willner, B. Willner, in: H. Morrison (Ed.), Bioorganic Photochemistry, Wiley, New York, 1993, pp. 1–110.
[8] R.C. Bertelson, in: J.C. Crano, R. Guglielmetti (Eds.), Organic Photochromic and Thermochromic Compounds, Plenum Press, New York, 1999, p. 11.
[9] J. Griffiths, Chem. Soc. Rev. 1 (1972) 481.
[10] K. Venkataraman, The Chemistry of Synthetic Dyes, Academic Press, New York, 1956.
[11] F. Hamon, F. Djedaini-Pilard, F. Barbot, C. Len, Tetrahedron 65 (2009) 10105.
[12] G.S. Hartley, Nature (London) (1937) 281.
[13] G.S. Hartley, J. Chem. Soc. (1937) 633.
[14] H. Rau, Angew. Chem., Int. Ed. Engl. 12 (1973) 224.
[15] G. Tiberio, L. Muccioli, R. Berardi, C. Zannoni, ChemPhysChem 11 (2010) 1018.
[16] J. Dokić, M. Gothe, J. Wirth, M.V. Peters, J. Schwarz, S. Hecht, P. Saalfrank, J. Phys. Chem. A 113 (2009) 6763.
[17] H. Fliegl, A. Kohn, C. Hattig, R. Ahlrichs, J. Am. Chem. Soc. 125 (2003) 9821.
[18] H. Knoll, in: W. Horspool, F. Lenci (Eds.), CRC Handbook of Organic Photochemistry and Photobiology, CRC Press, Boca Raton, 2004, p. 1.
[19] Ellis V. Brown, G. Richard Granneman, J. Am. Chem. Soc. 97 (1975) 621.
[20] S. Kume, H. Nishihara, Dalton Trans. (2008) 3260.
[21] Y.-L. Rao, H. Amarne, S. Wang, Coord. Chem. Rev. 256 (2012) 759.

[22] M. Endo, K. Nakayama, Y. Kaida, T. Majima, Tetrahedron Lett. 44 (2003) 6903.
[23] J. Otsuki, K. Suwa, K. Narutaki, C. Sinha, I. Yoshikawa, K. Araki, J. Phys. Chem. A 109 (2005) 8064.
[24] J. Otsuki, K. Suwa, K.K. Sarker, C. Sinha, J. Phys. Chem. A 111 (2007) 1403.
[25] K.K. Sarker, S.S. Halder, D. Banerjee, T.K. Mondal, A.R. Paital, P.K. Nanda, P. Raghavaiah, C. Sinha, Inorg. Chim. Acta 363 (2010) 2955.
[26] K.K. Sarker, D. Sardar, K. Suwa, J. Otsuki, C. Sinha, Inorg. Chem. 46 (2007) 8291.
[27] K.K. Sarker, B.G. Chand, K. Suwa, J. Cheng, Inorg. Chem. 46 (2007) 670.
[28] P. Pratihar, T.K. Mondal, A.K. Patra, C. Sinha, Inorg. Chem. 48 (2009) 2760.
[29] D. Banerjee, U.S. Ray, Polyhedron 25 (2006) 1299.
[30] P. Bhunia, D. Banerjee, P. Datta, P. Raghavaiah, Alexandra M.Z. Slawin, John D. Woollins, J. Ribas, C. Sinha, Eur. J. Inorg. Chem. (2010) 311.
[31] S. Saha (Halder), B.G. Chand, J.-S. Wu, T.-H. Lu, P. Raghavaiah, C. Sinha, unpublished work.
[32] G.M. Sheldrick, SHELXS-97, University of Gottingen, Germany, 1997.
[33] G.M. Sheldrick, SHELXL-97, University of Gottingen, Germany, 1997.
[34] L.J. Farrugia, J. Appl. Crystallogr. 30 (1997) 565.
[35] A.L. Spek, PLATON, The Netherlands, 1999.